J. Am. Chem. Soc. **2001,** *123,* 2251−2254 2251

Hindered Inversion of Chiral Ion−Dipole Pairs

Antonello Filippi, Francesco Gasparrini, and Maurizio Speranza*

Contribution from the Dipartimento di Studi di Chimica e Tecnologia delle Sostanze Biologicamente Attive, Università degli Studi di Roma "La Sapienza", P.le A. Moro 5, I-00185 Roma, Italy

Received June 6, 2000

Abstract: *O*-Protonated *S*-(−)-1-phenyl-1-methoxyethane (**I**$_S$) has been generated in the gas phase by $(CH_3)_2Cl^+$ methylation of *S*-(−)-1-phenylethanol (**1**$_S$). Detailed information on the reorganization dynamics of the intimate ion−dipole pair (**II**$_S$), arising from **I**$_S$ by C−O bond dissociation, is inferred from the kinetic study of the intramolecular inversion of configuration of **I**$_S$ vs its dissociation to α-methylbenzyl cation (**III**) and CH_3OH. The behavior of **II**$_S$ in the gas phase is compared to that observed in aqueous solutions, where the loss of optical activity of **I**$_S$ is prevented by exchange of the leaving CH_3OH with the solvent shell. Hindered inversion of **I**$_S$ in solution is attributed to the operation of attractive interactions between the moving CH_3OH moiety and the solvent cage which inhibit internal return in the intimate ion−dipole pair **II**$_S$. Similar interactions do not operate in the solvolysis of ^{18}O-labeled **1**$_S$ in aqueous acids, whose loss of optical activity efficiently competes with exchange of the leaving $H_2{}^{18}O$ with the solvent shell.

Introduction

Despite the great interest on the role of intimate ion−dipole intermediates in solvolytic reactions, the dynamics of their reorganization in a solvent cage remains largely unknown.[1] Recent progress in this area is mainly due to detailed kinetic and mechanistic studies of the acid-catalyzed solvolysis of optically active 1-phenylalkanols and their methyl ethers.[2,3] The investigations were based on the competition between the loss of optical activity of the chiral substrate and the exchange of the leaving moiety (XOH in Scheme 1) with a molecule of solvent (for simplicity, the solvent cage is represented by H_2O in Scheme 1).

The rate of ^{18}O exchange between water and the chiral-labeled alcohols as a function of racemization has been extensively used as a criterion for discriminating the S_N2 from the S_N1 mechanisms of solvolysis. The expected ratio of exchange vs racemization rate is 0.5 for the S_N2 mechanism and 1.0 for a pure S_N1 process.[4] With chiral ^{18}O-enriched 1-phenylethanol in aqueous acids, this ratio is found to be equal to 0.84 ± 0.05. This value has been interpreted in terms of the kinetic pattern of Scheme 1 involving the reversible dissociation of the oxonium ion **I**$_S$ (XOH = $H_2{}^{18}O$) to the chiral intimate ion−dipole pair **II**$_S$ ($k_{-1} > k_{\mathrm{inv}}$). In **II**$_S$, the leaving $H_2{}^{18}O$ molecule does not equilibrate immediately with the solvent (i.e. $H_2{}^{16}O$), but remains closely associated with the ion. This means that k_{inv} is of the same order of magnitude as k_{diss}.[2] In contrast, the rate constant ratio of exchange vs racemization of chiral 1-phenyl-1-methoxyethane in acidic acetonitrile−water solutions is as large as 0.99. The closeness of this value to that of a pure S_N1 mechanism indicates that, in Scheme 1 (XOH = CH_3OH), either k_{inv} is many orders of magnitude lower than k_{diss} or, if not, that internal return is negligible ($k_{-1} \ll k_{\mathrm{inv}}$).[3] This kinetic ambiguity prevents identification of the actual factors hindering inversion in **II**$_S$ (XOH = CH_3OH).[5]

Scheme 1

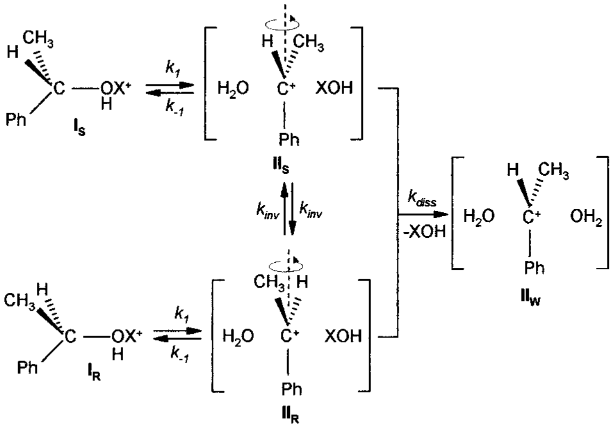

This paper is aimed at removing this ambiguity by comparing the behavior of optically active 1-phenylethanol and its methyl ethers in aqueous acids with that of their protonated derivatives in the gas phase. The absence of the solvent and the possibility of modulating in the gas phase the concentration of the added nucleophiles allow us to assess k_{inv} and k_{diss} without any perturbation from the reaction medium and incursion of spurious reaction pathways.[5] In addition, the comparison allows the determination of the effects of the aqueous solvent on the kinetics of Scheme 1.

The chiral oxonium ion **I**$_S$ (XOH = CH_3OH) is conveniently produced in the gas phase by methylating *S*-(−)-1-phenylethanol

---

(1) See, for instance: Richard, J. P.; Tsuji, Y. *J. Am. Chem. Soc.* **2000**, *122*, 3963 and references therein.

(2) (a) Merritt, M. V.; Bell, S. J.; Cheon, H. J.; Darlington, J. A.; Dugger, T. L.; Elliott, N. B.; Fairbrother, G. L.; Melendez, C. S.; Smith, E. V.; Schwartz, P. L. *J. Am. Chem. Soc.* **1990**, *112*, 3560 and references therein. (b) Merritt, M. V.; Anderson, D. B.; Basu, K. A.; Chang, I. W.; Cheon, H. J.; Mukundan, N. E.; Flannery, C. A.; Kim, A. Y.; Vaishampayan, A.; Yens, D. A. *J. Am. Chem. Soc.* **1994**, *116*, 5551 and references therein.

(3) Thibblin, A. *J. Phys. Org. Chem.* **1993**, *6*, 287 and references therein.

(4) For a review, see: Samuel, D.; Silver, B. *Adv. Phys. Org. Chem.* **1965**, *3*, 128.

(5) The different behavior of chiral 1-phenylalkanols and their methyl ethers in acids has been attributed to the different lifetime of the relevant intermediates **II**$_S$ and their sensitivity to solvation effects. Incursion of bimolecular substitutions and elimination−addition pathways may play a role as well (refs 2 and 3).

10.1021/ja001960o CCC: \$20.00

Scheme 2

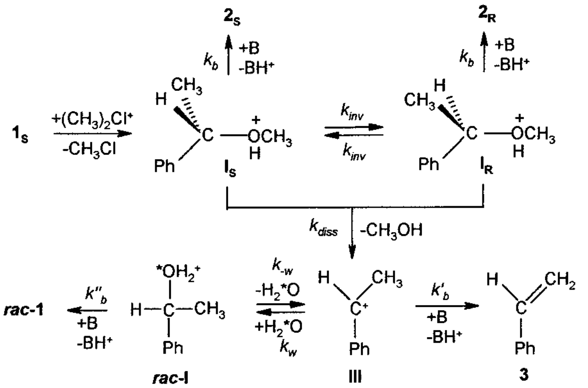

(1_S) with $(CH_3)_2Cl^+$ ions (Scheme 2). The latter ions are generated by γ-radiolysis of CH_3Cl, present as a bulk component (720 Torr) of gaseous mixtures containing traces of the alcoholic substrate, of $H_2{}^{18}O$, of a radical scavenger (i.e. O_2), and of a powerful base (i.e. $(C_2H_5)_3N$). This procedure allows formation of $\mathbf{I_S}$ (XOH = CH_3OH) in a gaseous inert medium (CH_3Cl) at pressures high enough to ensure its complete thermalization.

Experimental Section

Materials. Methyl chloride and oxygen were high-purity gases from UCAR Specialty Gases N. V., used without further purification. $H_2{}^{18}O$ (^{18}O-content > 97%) and $(C_2H_5)_3N$ were purchased from ICON Services. *S*-(−)-1-Phenylethanol (**1**$_\mathbf{S}$), its *R*-enantiomer (**1**$_\mathbf{R}$), and styrene (**3**) were research grade chemicals from Aldrich Co. Alcohol **1**$_\mathbf{S}$, used as starting substrate, was purified by enantioselective semipreparative HPLC on a chiral column of (*R*,*R*)-Ulmo (5 μm, 250 × 4.6 mm i.d.), eluent 99/1 (v/v) *n*-hexane/propan-2-ol, flow rate 1.0 mL min^{-1}; detection by UV (254 nm) and ORD (polarimeter) in series [$k_1'(-) = 3.64$; α=1.09; T 25 °C] and by enantioselective HRGC: (i) MEGADEX DACTBS-β (30% 2,3-di-O-acetyl-6-O-*tert*-butyldimethylsilyl-β-cyclodextrin in OV 1701; 25 m long, 0.25 mm i.d, d_f 0.25 μm) fused silica column, at $60 < T < 170$ °C, 4 °C min^{-1}; (ii) MEGADEX 5 (30% 2,3-di-*O*-methyl-6-*O*-pentyl-β-cyclodextrin in OV 1701; 25 m long, 0.25 mm i.d, d_f 0.25 μm) fused silica column at T = 125 °C. *S*-(−)-1-Phenyl-1-methoxyethane (**2**$_\mathbf{S}$) and its *R*-enantiomer (**2**$_\mathbf{R}$) were synthesized from the corresponding alcohols by the dimethyl sulfate method.[6] Their identity was verified by classical spectroscopic methods.

Procedure. The gaseous mixtures were prepared by conventional techniques, with the use of a greaseless vacuum line. Alcohol **1**$_\mathbf{S}$ (0.5−0.6 Torr), $H_2{}^{18}O$ (2−3 Torr), the radical scavenger O_2 (4 Torr), and the powerful base B = $(C_2H_5)_3N$ (1.2 Torr; proton affinity (PA) = 234.7 kcal mol^{-1})[7] were introduced into carefully outgassed 130 mL Pyrex bulbs, each equipped with a break-seal tip. The bulbs were filled with CH_3Cl (720 Torr), cooled to the liquid-nitrogen temperature, and sealed off. The irradiation were carried out at constant temperatures ranging from 25 to 160 °C with a ^{60}Co source to a dose of 2×10^4 Gy at a rate of 1×10^4 Gy h^{-1}, as determined by a neopentane dosimeter. Control experiments, carried out at doses ranging from 1×10^4 to 1×10^5 Gy, showed that the relative yields of products are largely independent of the dose. The radiolytic products were analyzed by GLC, with a Perkin-Elmer 8700 gas chromatograph equipped with a flame ionization detector, on the same columns used to analyze the starting alcohol **1**$_\mathbf{S}$. The products were identified by comparison of their retention volumes with those of authentic standard compounds and their identity confirmed by GLC-MS, using a Hewlett-Packard 5890 A gas chromatograph in line with a HP 5970 B mass spectrometer. Their yields were determined from the areas of the corresponding eluted peaks, using the internal standard (i.e. benzyl alcohol) method and individual calibration factors to correct for the detector response. Blank experiments were carried out to exclude the occurrence of thermal decomposition and racemization of the starting alcohol as well as of its ethereal products **2**$_\mathbf{S}$ and **2**$_\mathbf{R}$ within the temperature range investigated.

The extent of ^{18}O incorporation into the radiolytic products was determined by GLC-MS, setting the mass analyzer in the selected ion mode (SIM). The ion fragments at *m/z* 121 ($^{16}O - [M - CH_3]^+$) and 123 ($^{18}O - [M - CH_3]^+$) were monitored to analyze the **2**$_\mathbf{S}$ and **2**$_\mathbf{R}$ ethers. The corresponding alcohols **1**$_\mathbf{S}$ and **1**$_\mathbf{R}$ were examined by using the fragments at *m/z* 107 ($^{16}O - [M - CH_3]^+$ content) and 109 ($^{18}O - [M - CH_3]^+$).

Computational Details. Quantum chemical calculations were performed with use of an IBM RISC/6000 version of the GAUSSIAN 94 set of programs.[8] The 6-31G* basis set was used for all the atoms to optimize the geometries of the investigated species at the density functional level of theory, using the B3LYP functional which combines Becke's three-parameter hybrid description of exchange and the correlation functional of Lee, Yang, and Parr.[9] At the same level of theory, frequency calculations were performed for all the optimized structure to ascertain their minimum or transition state nature. Thermal contribution to enthalpy at 298 K and 1 atm, which include the effects of translation, rotation, and vibration, was evaluated by classical statistical thermodynamics within the approximation of ideal gas, rigid rotor, and harmonic oscillator behavior and using the recommended scale factor (0.994) for frequencies and zero-point energy correction. The intrinsic reaction coordinate (IRC) procedure[10] has been used to ascertain that the transition structures, identified on the potential energy hypersurface, are directly and continuously linked to the corresponding energy minima.

Results and Discussion

The main products from γ-radiolysis of the gaseous CH_3Cl/*S*-(−)-1-phenylethanol (**1**$_\mathbf{S}$) systems are *S*-(−)-1-phenyl-1-methoxyethane (**2**$_\mathbf{S}$), *R*-(+)-1-phenyl-1-methoxyethane (**2**$_\mathbf{R}$), styrene (**3**), and the 1-phenylethanol racemate (*rac*-**1**).[11] Their relative yields are listed in Table 1 under the $\mathbf{Y_{2S}}$, $\mathbf{Y_{2R}}$, $\mathbf{Y_3}$, and $\mathbf{Y}_{rac-\mathbf{1}}$[12] headings, respectively. The figures in the table represent the mean yield factors of the products, as obtained from several separate irradiations carried out under the same experimental conditions and whose reproducibility is expressed by the uncertainty level quoted. The ionic origin of the products is demonstrated by the sharp decrease (over 80%) of their abundance as the $(C_2H_5)_3N$ concentration is raised from ca. 0.1 to ca. 0.5 mol %.

No appreciable incorporation of the ^{18}O label is observed in the ethereal products **2**$_\mathbf{S}$ and **2**$_\mathbf{R}$, whereas the ^{18}O-content in racemate *rac*-**1** amounts to ~40%. The lack of any significant incorporation of the ^{18}O label into the ethereal products **2**$_\mathbf{S}$ and **2**$_\mathbf{R}$ excludes the involvement of water at any stage of their formation and points to the radiolytic $(CH_3)_2Cl^+$ ions as their exclusive precursors. The predominance of ether **2**$_\mathbf{S}$ over its enantiomer **2**$_\mathbf{R}$ under all conditions indicates that $(CH_3)_2Cl^+$

---

[6] Achet, D.; Rocrelle, D.; Murengezi, I.; Delmas, A.; Gaset, A. *Synthesis* **1986**, 643.

[7] Lias, S. G.; Hunter, E. P. L. *J. Phys. Chem. Ref. Data* **1998**, *27*, 413.

[8] Frish, M. J.; Trucks, G. W.; Schlegel, H. B.; Gill, P. M. W.; Johnson, B. G.; Robb, M. A.; Cheeseman, J. R.; Keith, T. A.; Petersson, G. A.; Montgomery, J. A.; Raghavachari, K.; Al-Laham, M. A.; Zakrzewski, V. G.; Ortiz, J. V.; Foresman, J. B.; Cioslowski, J.; Stefanov, B. B.; Nanayakkara, A.; Challacombe, M.; Peng, C. Y.; Ayala, P. Y.; Chen, W.; Wong, M. W.; Andres, J. L.; Repogle, E. S.; Gomperts, R.; Martin, R. L.; Fox, D. J.; Binkley, J. S.; Defrees, D. J.; Baker, J.; Stewart, J. P.; Head-Gordon, M.; Gonzales, C.; Pople, J. A. *Gaussian 94, Revision C. 2*; Gaussian, Inc.: Pittsburgh, PA, 1995.

[9] (a) Becke, A. D. *J. Chem. Phys.* **1993**, *98*, 1372, 5648. (b) Lee, C.; Yang, W.; Parr, R. G. *Phys. Rev. B* **1988**, *37*, 785.

[10] Gonzales, C.; Schlegel, H. B. *J. Phys. Chem.* **1990**, *94*, 5523.

[11] The irradiated systems invariably contain $H_2{}^{16}O$, as ubiquitous impurity either initially introduced in the mixture together with its bulk component or formed from its radiolysis. As pointed out previously (Troiani, A.; Gasparrini, F.; Grandinetti, F.; Speranza, M. *J. Am. Chem. Soc.* **1997**, *119*, 4525. Speranza, M.; Troiani, A. *J. Org. Chem.* **1998**, *63*, 1020), the average stationary concentration of $H_2{}^{16}O$ in the radiolytic systems is estimated to approach that of the added $H_2{}^{18}O$ (ca. 2−3 Torr).

Table 1. Gas-Phase Inversion vs Dissociation of *O*-Protonated (*S*)-(−)-1-Phenyl-1-methoxyethane $\mathbf{I_S}$[a]

reactn temp (°C)	yield factor[b] $\mathbf{Y_{2R}}$	$\mathbf{Y_{2S}}$	$\mathbf{Y_3}$	$\mathbf{Y}_{rac\text{-}\mathbf{1}}$	rate constants, ($\times 10^{-6}$ s^{-1})[c] k_{inv}	k_{diss}
25	0.015	0.960	0.005	0.020	0.7	1.2
60	0.047	0.837	0.042	0.074	2.4	5.4
85	0.096	0.716	0.068	0.120	5.4	8.3
100	0.085	0.556	0.116	0.243	5.9	17.1
120	0.082	0.335	0.299	0.284	8.9	31.2
140	0.079	0.191	0.421	0.309	15.2	45.1
140	0.061	0.156	0.468	0.315	14.2	52.7
160	0.030	0.054	0.615	0.301	20.2	79.9

[a] CH_3Cl: 720 Torr. O_2: 4 Torr. $H_2{}^{18}O$: 2−3 Torr. $(C_2H_5)_3N$: 1.2 Torr. Radiation dose: 2 × 10^4 Gy (dose rate: 1 × 10^4 Gy h^{-1}). [b] Each value is the average of several determinations, with an uncertainty level of ca. 5%; $\mathbf{Y}_{rac\text{-}\mathbf{1}}$ estimated by doubling the yield of (*R*)-(+)-1-phenylethanol (ref 12). [c] See text.

attacks the O-center of alcohol $\mathbf{1_S}$ yielding primarily the oxonium intermediate $\mathbf{I_S}$ with the same configuration of the starting substrate. Formation of alkene **3** and of the partially labeled *rac*-**1** mixture[13] is attributed to the partial unimolecular[14] dissociation of $\mathbf{I_S}$ into the α-methylbenzyl cation (**III**) and CH_3OH prior to its neutralization by the strong base B = $(C_2H_5)_3N$.

Accordingly, formation of the products of Table 1 conforms to the reaction network of Scheme 2. Its kinetic treatment leads to the following equations: [15]

$$\mathbf{Y_{2S}} = 0.5[e^{-k_{diss}\tau} + e^{-(2k_{inv} + k_{diss})\tau}] \quad (1)$$

$$\mathbf{Y_{2R}} = 0.5[e^{-k_{diss}\tau} - e^{-(2k_{inv} + k_{diss})\tau}] \quad (2)$$

$$\mathbf{Y_2} + \mathbf{Y}_{rac\text{-}\mathbf{1}} = 1 - e^{-k_{diss}\tau} \quad (3)$$

The k_{inv} and k_{diss} rate constants, derived from eqs 1−3, are expressed as:

$$k_{inv} = 0.5\tau^{-1}\{\ln[(\mathbf{Y_{2S}} + \mathbf{Y_{2R}})/(\mathbf{Y_{2S}} - \mathbf{Y_{2R}})]\} \quad (4)$$

$$k_{diss} = \tau^{-1}\{\ln[1 - (\mathbf{Y_3} + \mathbf{Y}_{rac\text{-}\mathbf{1}})]^{-1}\} \quad (5)$$

The τ term represents the lifetime of ions $\mathbf{I_S}$ and $\mathbf{I_R}$ prior to deprotonation by the base B = $(C_2H_5)_3N$. Taking equal to unit the efficiency of the ion deprotonation by B (e.g. k_b in Scheme 2), τ is expressed by $(k_b[B])^{-1}$.[16] The Arrhenius plots of k_{inv} and k_{diss} over the 25−160 °C temperature range are reported in Figure 1. The linear curves obey the following equations:

$$\log k_{inv} = (10.4 \pm 0.1) - [(6.2 \pm 0.2) \times 10^3]/2.303RT \quad (r^2 = 0.994) \quad (6)$$

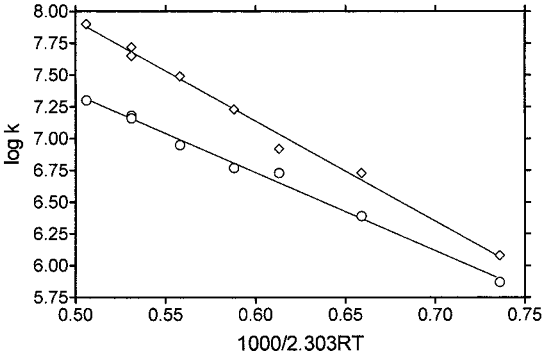

Figure 1. Arrhenius plots for the $\mathbf{I_S} \leftrightarrows \mathbf{I_R}$ intracomplex rearrangement (circles) and the $\mathbf{I_S} \rightarrow \mathbf{III} + CH_3OH$ dissociation (diamonds).

$$\log k_{diss} = (11.9 \pm 0.3) - [(7.9 \pm 0.2) \times 10^3]/2.303RT \quad (r^2 = 0.992) \quad (7)$$

The relevant activation parameters, calculated from the transition-state theory equation, are the following: $\Delta H^{\ddagger}_{inv} = 5.4 \pm 0.3$ kcal mol^{-1} and $\Delta S^{\ddagger}_{inv} = -13.3 \pm 1.0$ cal mol^{-1} K^{-1}; $\Delta H^{\ddagger}_{diss} = 7.1 \pm 0.3$ kcal mol^{-1} and $\Delta S^{\ddagger}_{diss} = -6.7 \pm 1.2$ cal mol^{-1} K^{-1}.

The values in Table 1 indicate that, at all temperatures investigated, k_{inv} is *anything but negligible* relative to k_{diss}, being just 2−4 times lower. This implies that, in acidic media, the hindered inversion of $\mathbf{I_S}$ (XOH = CH_3OH) has to be ascribed to the lack of appreciable $\mathbf{II_S} \rightarrow \mathbf{I_S}$ (and $\mathbf{II_R} \rightarrow \mathbf{I_R}$) internal return ($k_{-1} \ll k_{inv}$; Scheme 1), rather than to k_{inv} negligible relative to k_{diss}.[3] Accordingly, the difference in the behavior of $\mathbf{II_S}$ (and $\mathbf{II_R}$) in acidic solution essentially reduces to $k_{-1} > k_{diss}$, when XOH = $H_2{}^{18}O$, and $k_{-1} \ll k_{diss}$, when XOH = CH_3OH.

A reason for such a difference has to be sought in the relevant $\mathbf{I_S} \rightarrow \mathbf{I_R}$ transition structures and their position along the reaction coordinate.

Quantum-chemical calculations at the B3LYP/6-31G* level have been employed to gather information on this point.[17] The structures and 298 K relative enthalpies of the critical points identified on the $[C_6H_5CH^+CH_3,CH_3OH]$ hypersurface are illustrated in Figure 2. The first-order critical points $\mathbf{TS_1}$ and $\mathbf{TS_2}$ represent two transition structures of the $\mathbf{I_S} \rightarrow \mathbf{I_R}$ inversion reaction. Taking into account the intrinsic limitations of the B3LYP functional in describing noncovalent interactions and the necessarily limited dimensions of the 6-31G* basis set employed, the $\mathbf{I_S} \rightarrow \mathbf{I_R}$ (XOH = CH_3OH) activation enthalpies computed at 298 K (2 ($\mathbf{TS_1}$) and 4 kcal mol^{-1} ($\mathbf{TS_2}$)) are not inconsistent with that obtained experimentally ($\Delta H^{\ddagger}_{inv} = 5.4 \pm 0.3$ kcal mol^{-1}). According to Figure 2, the $\mathbf{TS_1}$ and $\mathbf{TS_2}$ geometries show a pronounced C_α−O bond distance between the leaving CH_3OH molecule and the planar carbocation **III** (2.86 and 3.55 Å, respectively). The moving CH_3OH moiety is much closer to the acidic hydrogens of **III** than to its C_α center. This suggests that hydrogen bond interactions between CH_3OH and the acidic hydrogens of **III** play a major role in $\mathbf{TS_1}$ and $\mathbf{TS_2}$, whose structure resembles more those of the intermediates **IV** and **V**, respectively, than that of the starting oxonium ion $\mathbf{I_S}$. This view is corroborated by the relevant experimental data. The negative $\Delta S^{\ddagger}_{inv}$ value is a symptom of the stiffness of the transition structures $\mathbf{TS_1}$ and $\mathbf{TS_2}$ due to the coordination of the CH_3OH molecule between two hydrogens of the planar carbocation **III** and to the restricted rotation of its

---

(12) Owing to the presence of the starting alcohol $\mathbf{1_S}$, the extent of $\mathbf{II_S} \rightarrow \mathbf{I_S}$ association cannot be directly determined. However, GLC-MS analysis reveals the formation of ^{18}O-labeled $\mathbf{1_S}$ in concentrations equal to that of the ^{18}O-labeled enantiomer $\mathbf{1_R}$. On these grounds, the overall abundance of $\mathbf{1_S}$ can be taken as equal to that of $\mathbf{1_R}$ and, therefore, the yield factor of *rac*-**1** can be estimated by doubling that of $\mathbf{1_R}$.

(13) The conceivable bimolecular $H_2{}^{18}O$-to-CH_3OH displacement on $\mathbf{I_S}$ as a route to racemate *rac*-**1** is ruled out on both stereochemical and thermochemical grounds. For instance, H_2O-to-CH_3OH substitution on O-protonated benzyl methyl ether is 14.4 kcal mol^{-1} endothermic.

(14) Kinetic predominance of proton transfers vs *β*-eliminative processes allows us to assign the formation of **3** to deprotonation of **III** by $(C_2H_5)_3N$.

(15) Andraos, J. *J. Chem. Educ.* **1999**, *76*, 1578.

(16) The collision constant k_b between $\mathbf{II_S}$ and $(C_2H_5)_3N$ is calculated according to: Su, T.; Chesnavitch, W. J. *J. Chem. Phys.* **1982**, *76*, 5183.

(17) Owing to the molecular complexity of the species involved, any description of the $[C_6H_5CH^+CH_3, CH_3OH]$ hypersurface at a more sophisticated level of theory is computationally unfeasible.

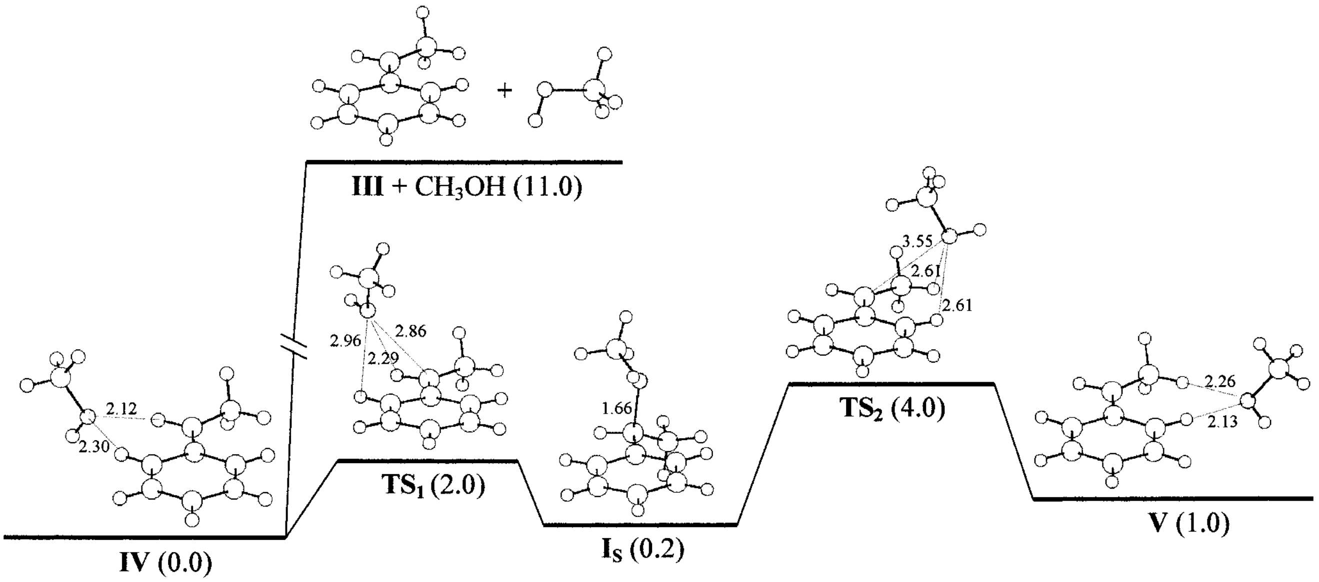

Figure 2. B3LYP/6-31G*-optimized geometries and 298 K relative enthalpies (in kcal mol^{-1}) of the critical structures on the [$C_6H_5CH^+CH_3$,CH_3-OH] hypersurface.

alkyl groups. Furthermore, the late character of the **TS$_1$** and **TS$_2$** transition structures is supported by the observation that the measured $\Delta H^{\ddagger}_{inv}$ value is not much lower than the $\Delta H^{\ddagger}_{diss}$ one.

In the solvolysis of **1$_S$** in aqueous acids (Scheme 1), the removed CH_3OH molecule in **TS$_1$** and **TS$_2$** is close enough to the solvent cage to feel the effects of electrostatic interactions with the H_2O molecules. These attractive electrostatic forces are expected to lower the **II$_S$** → **II$_W$** dissociation barrier relative to that of the **II$_S$** → **I$_S$** internal return which should feel much less the effects of the solvent shell ($k_{-1} < k_{diss}$ in Scheme 1).[3]

Taking into account the factors governing inversion of configuration in the strictly related chiral allylic alcohols in the gas phase[18,19] and in solution,[2,3] the **I$_S$** → **I$_R$** (XOH = $H_2{}^{18}O$) transition structure is instead expected to be placed much earlier along the reaction coordinate so as to resemble the starting **I$_S$** ion more than the hydrogen-bonded intermediates corresponding to **IV** and **V** of Figure 2. In it, the moving $H_2{}^{18}O$, less basic than CH_3OH,[7] sits nearby the departure face of the still flexible benzylic residue and does not appreciably interact with its acidic hydrogens. A surplus of energy is needed to remove the $H_2{}^{18}O$ moiety far enough to establish appreciable interactions with the solvent cage and to promote **II$_S$** → **II$_W$** dissociation. As a consequence, **II$_S$** → **I$_S$** internal return can efficiently compete with $H_2{}^{18}O$ diffusion to the aqueous cage ($k_{-1} > k_{diss}$). Besides, the shielding effect of the $H_2{}^{18}O$ leaving group accounts for the observed prevalence of the inversion of configuration in the H_2O-to-$H_2{}^{18}O$ exchange in solution.[2]

In conclusion, hindered inversion of **I$_S$** (XOH = CH_3OH) in solution is attributed to the operation of attractive interactions between the moving CH_3OH moiety and the solvent cage which inhibit internal return in the intimate ion−dipole pair **II$_S$** (XOH = CH_3OH). Similar interactions do not operate in the solvolysis of ^{18}O-labeled **1$_S$** in aqueous acids, whose loss of optical activity efficiently competes with exchange of the leaving $H_2{}^{18}O$ with the solvent shell.

Acknowledgment. This work was supported by the Ministero della Università e della Ricerca Scientifica e Tecnologica (MURST) and the Consiglio Nazionale delle Ricerche (CNR).

JA001960O

---

[18] Troiani, A.; F.Gasparrini, F.; Grandinetti, F.; Speranza, M. *J. Am. Chem. Soc.* **1997**, *119*, 4525.

[19] Troiani, A.; Speranza, M. *J. Org. Chem.* **1998**, *63*, 1012.